

Pleural Fluid GSDMD is a Novel Biomarker for the Early Differential Diagnosis of Pleural Effusion

Pu Li (✉ lipu@hospital.cqmu.edu.cn)

Department of Laboratory Medicine, the Second Hospital of Chongqing Medical University, 8602363693193, Chongqing 400010, China. <https://orcid.org/0000-0002-9152-3143>

Jing Shi

Chongqing Medical University First Affiliated Hospital

Lijing Zhou

Chongqing Medical University second Affiliated Hospital

Bo Wang

Chongqing Medical University Second Affiliated Hospital

Lijun Zhang

Chongqing Medical University Second Affiliated Hospital

Liang Duan

Chongqing Medical University Second Affiliated Hospital

Qin Hu

Chongqing Medical University Second Affiliated Hospital

Xiaolan Zhou

Chongqing Medical University Second Affiliated Hospital

Yuan Yuan

Chongqing Medical University

Dandan Li

Chongqing Medical University Second Affiliated Hospital

Hong Chen

Chongqing Medical University Second Affiliated Hospital

Qing Zhao

Chongqing Medical University Second Affiliated Hospital

Xuemei Peng

Chongqing people's hospital

Weixian Chen

Chongqing Medical University Second Affiliated Hospital

Keywords: GSDMD, Pyroptosis, Pleural Effusion, Nucleated cells, Biomarker

Posted Date: September 8th, 2020

DOI: <https://doi.org/10.21203/rs.3.rs-66873/v1>

License:  This work is licensed under a Creative Commons Attribution 4.0 International License.

[Read Full License](#)

Abstract

Introduction: To accurate differential diagnosis of pleural effusion (PE) is still a big challenge. Gasdermin D (GSDMD), controlling pyroptosis in cells, has multiple physiological functions. The diagnostic role of GSDMD in PE remains unknown.

Methods: Sandwich ELISA kits that we developed were applied to measure the level of GSDMD for 335 patients with the definite cause of PE, including transudative pleural effusion, tuberculous pleural effusion (TPE), parapneumonic pleural effusion (PPE), and malignant pleural effusion (MPE). Clinical follow up of 40 cases of PPE were conducted and divided into efficacy group and non-efficacy group according to therapeutic outcome. The receiver operating characteristic (ROC) curve was conducted to explore the diagnostic and predictive performance of GSDMD. Nucleated cells (NCs) in pleural effusion were isolated and further infected with bacteria to verify the cell source of GSDMD.

Results: In this study, there was prominent statistical significance among the concentration of GSDMD in these four groups (all $p < 0.0001$, except between MPE and PPE). ROC curve indicated that GSDMD can be an efficient biomarker for differential diagnosis of transudative pleural effusion and other groups (all AUC ≥ 0.973). Noteworthily, the highest AUC belonged to tuberculosis diagnosis of 0.990, and the sensitivity and specificity were 100% and 97.53%. The combination of GSDMD, adenosine deaminase (ADA) and lactate dehydrogenase (LDH) will further improve the diagnostic efficiency especially between TPE and PPE (AUC = 0.968). The AUC of GSDMD change at day 4 could predict the therapeutic effect at an early stage was 0.945 ($P < 0.0001$). Interestingly, bacterial infection experiments further confirm that the pleural fluid GSDMD was expressed and secreted mainly by the NCs.

Conclusion: GSDMD and its combination not only candidate as the potentially novel biomarkers to separate PEs early and effectively, but also monitor disease progression.

Introduction

Pleural effusion (PE) occurs frequently in respiratory medicine patients. PE accumulation develops when pathological processes result in an imbalance between fluid formation and absorption, including systemic conditions, lung diseases, and organic dysfunction and so on. Tuberculous pneumonia, lung infection and malignant-pulmonary diseases are the most common causes of pleural effusion [1].

The formation of an exudate usually implies pleural disease and biochemical analysis of PE is widely employed in clinical samples to distinguish the cause of PE. Considered as the golden standard, the microscopic examination of *Mycobacterium tuberculosis* (Mtb) has limited sensitivity and the culture of Mtb in the pleural fluid has to be prolonged for several weeks and requires higher laboratory conditions. Lactate dehydrogenase (LDH), measured in pleural fluid, is implicated in parapneumonic effusion, tuberculous pleuritis or malignant effusion, thus it is less specific and sensitive in distinguishing the cause of PE [2]. Measurement of ADA will contribute to the diagnosis of tuberculous pleural effusion (TPE). With 63 studies, a meta-analysis of diagnostic capacity about ADA in tuberculous pleurisy showed

that mean sensitivity and specificity were 0.92 and 0.90, respectively [3]. Despite the stable cut-off value and well-established standard method and operating protocol of ADA, a recent study found that it can be an independent predictor of worse survival in patients with malignant pleural effusion (MPE). Higher and lower ADA level is correlated with worse survival when compared to a normal level, indicating the level of ADA may not have obvious diagnostic performance in antidiastole of TPE and MPE, although it passes great diagnostic efficiency of pleural tuberculosis [4]. In addition, criticism about the diagnostic performance of ADA in a low prevalence setting has been made [5]. More cost-effective, high-performance and method-feasible biomarkers should be explored.

Pyroptosis is a form of inflammatory programmed cell death pathway [6] activated by caspase-1 or caspase-11/4/5, which cleave gasdermin D (GSDMD) to generate a gasdermin-N domain (NT-GSDMD) and induce the activation and secretion of the two prominent pro-inflammatory cytokines, interleukin-1 β (IL-1 β) and IL-18 [7]. GSDMD, a 480-amino acid protein, consists of a C-terminal inhibition domain and an N-terminal pore-forming domain which eventually oligomerizes and perforates the plasma membrane that drives pyroptosis [8]. There exists a cleavage site between the two domains, D276 of mouse and D275 of humans [9]. Studies have shown that, in non-small cell lung cancer (NSCLC), pneumonia and pulmonary tuberculosis, the GSDMD level was significantly upregulated [10-12].

Quantitative detection of GSDMD in PE hasn't been reported yet, and so far, it remains elusive about the relationship between levels of GSDMD and PE-related diseases. In this study, we made efforts to evaluate the value of GSDMD as a novel parameter to the differential diagnosis of pleural fluid, and get a better insight into the relationship between the levels of pleural fluid GSDMD and the count of Nucleated cells (NCs).

Materials And Methods

Study Population

Admitted to the Second Affiliated Hospital of Chongqing Medical University, between October 2017 and November 2019, a total of 335 samples collected from clinical patients in respiratory medicine were divided into four groups, including 81 cases of transudative pleural effusion (the control group), 82 cases of TPE, 80 cases of MPE, and 92 cases of parapneumonic pleural effusion (PPE). Clinical follow-up of 40 cases of PPE with Gram-negative bacteria infection would have been done to define if the change of PE-GSDMD might inform about the efficacy evaluation of pneumonia. TPE and MPE samples obtained from tuberculous pleurisy and NSCLC patients, respectively. Tuberculous pleurisy was diagnosed by the tuberculosis guidelines for the diagnosis and treatment of tuberculosis in the global tuberculosis report. Patients with NSCLC were in term of the diagnosis and treatment guide, issued by the National Comprehensive Cancer Network (NCCN). Patients coupling with lung cancer and tuberculous pneumonia were excluded from this study. The PPE patients were based on the criteria: (1) exudates were linked with bacterial pneumonia, lung abscesses, or bronchiectasis; (2) people who manifest as inflammatory pleuritis, chronic empyema, or pleural fibrosis and plaques, without Mtb can be observed in pleural fluid.

Transudative pleural effusions that did not belong to any of the categories described above were classified in the 'transudate' group. This study was performed according to the principles of the Declaration of Helsinki and was approved by the medical ethics committee of the Second Affiliated Hospital of Chongqing Medical University. The clinical characteristics of the subject in the study were presented in table 1.

PE was collected according to the standard operating protocol and was immediately transferred to the clinical laboratory. Pleural fluid was then centrifuged at 1500 rpm for 10 min at room temperature, supernatants were collected and stored at -80°C for later analysis. IFN- γ levels were detected by an ELISA kit (WANTAI BioPharm, Beijing, China) following the manufacturer's protocols. The activity of ADA and LDH was detected by Hitachi Modular 7600 chemistry analyzer (Hitachi, Tokyo, Japan) with the test kit (Maccura, Sichuan, China). IL-1 β was detected by IMMULITE® 1000 chemiluminescence immunoassay analyzer (Siemens, Germany). The nucleated cells (NCs) count in pleural fluid was quantitatively analyzed by Sysmex XT4000i Automatic Blood Analyzer (Sysmex, Kobe, Japan).

NCs Isolate and Cell Infection

NCs were isolated aseptically using the Ficoll-Hypaque gradient centrifugation method from pleural effusion and cultured in RPMI-1640 supplement in 6-well plates (10^6 cells/well). In our experiments, *Escherichia coli* (*E.coil*), *Staphylococcus aureus* (*S.aureus*), *Salmonella* and *Pseudomonas aeruginosa* (PA) were added into the culture respectively (bacterium: cell=30:1). At various time points of 0h (control), 1h, 2h, 4h, 8h, 16h, 24h and 48h, supernatants were harvested for determining GSDMD concentrations. At the same time, determine the intracellular GSDMD proteins at the various time points of 0h (Control), 1h, 2h, 4h and 8h. And we also detected the concentration of LDH, IL-1 β and IFN- γ at time points of 0h (Control), 1h, 2h, 4h, 8h in culture supernatants at the presence of *E.coil*, *S.aureus*, PA and *Salmonella*.

PE-GSDMD in patients who would have a response or stable disease to antibiotic

This was a non-intervention study. The suspected infected patients were given empirical anti-infection treatment for the first time. The drug selection was based on the guidelines [13] and epidemiology, and was adjusted according to the clinical response and/or drug sensitivity after the initial efficacy evaluation. The course of treatment combined with guidelines [13] and treatment response. GSDMD samples were collected in the baseline, day 2 and day 4 in the duration of therapy. The efficacy evaluation was assessed and divided into efficacy and non-efficacy at the end of treatment by a group of three or more doctors according to the guiding principle of clinical trials on anti-bacterial drugs by the Ministry of Health [14]. Clinical efficacy, microbiological efficacy and the comprehensive curative effect were included in the evaluation criteria but without GSDMD.

Analysis of Pleural Fluid GSDMD

GSDMD was measured by an ELISA method as we previously described [15]. In short, 100 μ L of serum samples or standard (recombinant Human GSDMD protein; Abcam, USA) were added into each capture

antibody-coated well (anti-GSDMD antibody; Abcam, USA) and incubated 1 hour at 37°C. After aspirating and washing each well 3 times, 100 µL of diluted detection antibody-conjugated HRP (rabbit anti-human IgG H&G antibody; Abcam, USA) was added and incubated 30 mins at 37°C. Repeating the aspiration/wash of each well 3 times, 100 µL of substrate solution was added and incubated at room temperature for 30 mins. Next, adding 50 µL of stop solution (1 mol/L H₂SO₄) to each well. The absorbance of the colored solution of GSDMD was measured at 450 nm by using a Multiskan™ FC microplate reader (Thermo Scientific, MA, USA).

Statistical Analysis

All statistical analysis was performed with SPSS software, version 16.0 (SPSS, Inc., Chicago, IL, USA). The clinical characteristics of patients were presented as means ± SD. Parametric tests were used since data were normally distributed as determined by a normality test. Comparison of continuous variables was made by Student's *t*-test. Differences among more than two groups were compared by one-way analysis of variance (one-way ANOVA). All tests in this study were two tails and *P*-value <0.05 was considered statistically significant. Receiver operator characteristic (ROC) curves were used to evaluate the diagnostic accuracy of GSDMD, LDH, ADA and the combination of three biomarkers. Sensitivity, specificity and the areas under ROC curves (AUC) was included.

Compliance with Ethics Guidelines

This article does not contain any studies performed by any of the authors with human participants or animals.

Results

Correlation analysis of GSDMD, ADA and LDH

As we discussed before, ADA and LDH biochemical analysis of PE is widely employed in clinical samples to distinguish the cause of PE. In the first part of our experiment, in order to find the correlation of GSDMD, a novel biomarker, and other usual biochemical indexes, we investigated the activity of ADA and LDH in these four groups. And then, we made correlation analyses among the level of GSDMD, ADA, and LDH. Interestingly, there was a statistically significant relationship among the three biomarkers when all patients with pleural exudates were considered. As shown in Figure 1, the results illustrated that GSDMD content in PE was positively correlated with ADA ($r = 0.4772$, $p < 0.0001$) and with LDH ($r = 0.2755$) ($p < 0.0001$) which indicated that GSDMD could turn into an effective biomarker for PE antidiastole.

Diagnostic value of GSDMD for PE antidiastole

We analyzed whether or not the level of GSDMD associated with a different kind of PE. Interestingly, there was conspicuous statistical significance among the concentration of GSDMD in these four groups ($p < 0.0001$), except between MPE and PPE ($P > 0.05$) (Figure 2A), but not of ADA and LDH (Figure 2B, C). The

capacity of GSDMD to differentiate PEs was assessed with ROC curve analyses (Table 2). GSDMD showed a pretty high diagnostic capacity for distinguishing transudative PE from TPE (AUC = 0.990), MPE (AUC = 0.963) and PPE (AUC = 0.967) (Figure 3), while the AUC of ADA was determined as 0.937, 0.896 and 0.771, and the AUC of LDH was determined as 0.872, 0.864 and 0.710, respectively (Table 2). With the highest level of AUC, the cut-off value, the sensitivity and specificity when GSDMD was used to differentiate TPE and transudative PE were 18.40 ng/mL, 100% and 97.53%, respectively. Additionally, for diagnostic sensitivity alone, compared with ADA and LDH, GSDMD was the highest for differentiating transudative pleural effusion from MPE, TPE, and PPE. Furthermore, GSDMD also did well in antidiastole between TPE and PPE (AUC = 0.885) and between TPE and MPE (AUC = 0.848). However, the diagnostic capacity of GSDMD was lower in the differential diagnosis between PPE and MPE.

Diagnostic value of combined detection of GSDMD, ADA and LDH for PE antidiastole

In clinical diagnosis, a combination of indexes is generally used to improve diagnostic efficiency. Like GSDMD, the combination of these three biomarkers displayed outstanding performance in the differential diagnosis between pleural transudate and TPE, with 100% sensitivity and 97.5% specificity (AUC = 0.998). Moreover, the combination exhibited higher diagnostic ability for antidiastole between pleural transudate and MPE (AUC = 0.980), between pleural transudate and PPE (AUC = 0.973), and between TPE and PPE (AUC = 0.968) (Table 3). What's more, there existed higher diagnostic specificity and sensitivity when using combined indexes than single.

Correlation between PE-GSDMD activity and efficacy of PPE treatment

PE-GSDMD of baseline, day 2 and day 4 in the duration of therapy evaluated in all patients in both groups. Mean PE-GSDMD of each point was significantly lower in efficacy group than non-efficacy group (baseline; $[35.28 \pm 18.72]$ ng/mL versus $[26.42 \pm 11.09]$ ng/mL [$p = 0.1138$], day 2 in the duration of therapy; $[27.72 \pm 14.53]$ ng/mL versus $[25.45 \pm 7.57]$ ng/mL [$p = 0.5898$], day 4 in the duration of therapy; $[15.25 \pm 12.48]$ ng/mL versus $[35.01 \pm 14.78]$ ng/mL [$p < 0.0001$], Table 4). The level of PE-GSDMD gradually declined from baseline during treatment in the efficacy group, while the non-efficacy group presented uptrend. A 18.82% and 59.15% decrease in PE-GSDMD from baseline was observed at day 2 and day 4 during therapy, respectively ($p = 0.0205$, $p < 0.0001$, Table 4). In predicting whether patients would have a response or stable disease to the antibiotic, the percentage change in PE-GSDMD at day 4 anticipated to have a diagnostic accuracy with AUC of 0.945 (78.57% sensitivity and 96.15% specificity) (Figure 4).

Correlation analysis of GSDMD and NCs

During the study, we found subjects with etiologies showed a notable elevation of total nucleated cell counts. As shown in Figure 5A, there was a significant statistical difference between pathological groups

and PE (Control) (all $P < 0.0001$), except between MPE and TPE ($P > 0.05$). Hence, we made a correlation analysis between the level of NCs and GSDMD. As expected, concentrations of GSDMD in tuberculous, malignant and parapneumonic PE all were correlated positively with numbers of pleural NCs ($r = 0.6615$; $P < 0.0001$) (Figure 5B), suggested that pleural fluid GSDMD might be produced mainly by these local NCs.

The results of cell infection in *vitro* culture

To further verify the source of GSDMD, NCs were isolated and cultured in *vitro* in the presence of *E.coil*, *S.aureus*, PA and *Salmonella*, respectively. As shown in Figure 6, all bacteria were capable of inducing GSDMD production from NCs in a time-dependent manner. At the time point of 2h, the concentration of secreted-GSDMD began increasing significantly, especially in the presence of *S.aureus* (a 20-fold increase compared with the control). As to the level of intracellular GSDMD, after one hour there was almost no growth. In Figure 7, we adopted trend analysis (fixed base dynamic ratio = assay value/fixed value) which adopted the concentration at 0h as fixed value to analyze variation tendency of the concentration of GSDMD, LDH, IFN- γ and IL-1 β in culture supernatants at the presence of *E.coil*, *S.aureus*, PA and *Salmonella*. With the extension of incubation time, the supernatant level of GSDMD, IL-1 β and LDH were significantly elevated after NCs incubating with bacteria. What's more, compared with LDH and IFN- γ but not with IL-1 β , GSDMD displayed superiority both in the time that biomarker began to grow and the degree of growth at the presence of *E.coil*, *S.aureus*, and *Salmonella*. Nevertheless, at the presence of PA, IFN- γ possessed the max fixed base dynamic ratio.

Discussion

To our knowledge, the current study was the first one to investigate the diagnostic value of GSDMD in differential diagnosing different kinds of PE (including pleural transudate, TPE, MPE, and PPE). Our results indicate that the concentration of GSDMD not only acts as a novel biomarker for differential diagnosis of pleural fluid with a high diagnostic sensitivity and disease progression prediction but also can combine with ADA and LDH to improve the diagnostic ability. Moreover, PE-GSDMD displayed drug efficacy monitoring. Additionally, we found GSDMD in PE was secreted by NCs, manifested by the correlation analysis and cell infection results.

Pyroptosis is a form of pathogen-induced and caspase-dependent cell death type characterized by the exposure of phosphatidylserine, pore-formation, cell membrane rupture and secretion of cytoplasmic contents, including IL-1 β , LDH and IL-18 [16]. Recent studies show that pyroptosis can be triggered by diverse pathological stimuli such as infectious disease, nervous system diseases and cancer. When the body is infected with bacteria, lipopolysaccharide (LPS) will combine caspase-4, caspase-5, and caspase-11, acting as cytosolic LPS receptors and induce cell pyroptosis [17, 18]. Similarly, through pyroptosis macrophage infected with Mtb can destroy the survival environment of Mtb, and eventually prevent Mtb replication [19, 20]. Mtb activated the canonical NLRP3 inflammasome by inducing potassium efflux

upon infection of monocytes and macrophages, followed by GSDMD-dependent pyroptosis [21]. NLRP3 and AIM2 are considered two crucial kinds of pattern recognition receptors (PRR) which can activate cell pyroptosis after recognizing pathogen-associated molecular patterns (PAMP) [22, 23]. According to a large number of reports, microRNA induction [24], chemotherapy drugs [25], LXRs receptor mediation [26] and other manners can induce the occurrence of pyroptosis of tumor cells. Thereinto, microRNA, approximately 21-23 nucleotides in length, can directly target caspase-1, thereby inhibiting tumor cell proliferation and migration [24].

A recent report displays that mediated by ESCRT III components, a calcium-dependent membrane repair machinery, can antagonize the execution phase of pyroptosis [9]. Calcium flux is an evolutionarily conserved trigger for cell membrane repair through exocytosis of vesicles such as lysosomes, mobilization of annexins, and recruitment of ESCRT machinery to sites of membrane injury [27]. Based on this membrane repair machinery, cell-free culture supernatants will detect GSDMD, as has been reported [28]. What's more, what could be detected in culture supernatants is GSDMD-NT, and GSDMD was only detected in the cell. Additionally, pyroptosis is a kind of cell lytic death way. After membrane rupture, GSDMD releases in large quantities. These are the reasons that GSDMD can be detected in pleural suffusion.

Biochemical testing of body fluid has been widely performed in the differential diagnosis between transudate and pathological pleural effusions. Though traditional biomarkers, such as ADA, LDH, glucose, protein, have been applied and new markers like IL-27 [29], IFN- γ [30], CXCL9 and CXCL11 [31] are been developing, ADA is still the most cost-effective pleural fluid marker. However, its value is questioned in antidiastole and a low prevalence setting. We have reported previously using proteome analysis for antidiastole of TPE and MPE [32]. In this study, we innovatively developed GSDMD, an indispensable molecular requirement in pyroptosis, as a novel biomarker for PE-related disease diagnosis and antidiastole of PE. GSDMD showed higher diagnostic accuracy than ADA and LDH in distinguishing transudate and other pathological pleural effusions, with 0.973 average level of the AUC for GSDMD, 0.868 for ADA, and 0.815 for LDH. It is worth to mentioning that the sensitivity and specificity for distinguishing transudate from TPE were 100% and 97.53% (AUC = 0.990), at the cut-off value of 18.40 ng/mL. What's more, GSDMD not only manifests predominant advantage in the antidiastole of TPE but also performs well in the antidiastole of TPE and PPE (AUC = 0.885), and TPE and MPE (AUC=0.848). To make better clinical practical performance, we also calculated the cut-off value for GSDMD was selected based on the highest diagnostic accuracy. Although there existed some deficiency of GSDMD in the differential diagnosis of pleural, such as the antidiastole of MPE and PPE, and TPE and PPE, it was indisputable that GSDMD had a good diagnose performance. Furthermore, the combination of the three indexes further improved the diagnostic ability.

As we mentioned before, GSDMD can be detected in PE as a sign of pyroptosis in theory. And interestingly there existed an arresting positive correlation between the concentration of GSDMD and the count of NCs, which suggested GSDMD might be secreted by these pleural local NCs. After NCs infected by bacteria, the level of GSDMD in culture supernatants presented a growth trend in a time-dependent

manner. Besides, with the extension of incubation time, a notable increase in IL-1 β and LDH, as the main feature of pyroptosis [33], could be observed. These are consistent with the previous findings that pyroptosis mainly occurs in monocytes, macrophages, and also neutrophils [34-35], to induce lytic cell death, release bacteria and expose them to reactive oxygen species (ROS) in neutrophils [36]. These data, on the one hand, confirmed a large number of GSDMD would be generated and secreted by NCs, on the other, after infection secreted-GSDMD released space and also increased with time, which made it an ideal inflammatory marker. Moreover, the invariability of the level of intracellular GSDMD after one hour may result of gasdermin pores have formed and cytoplasmic contents outflowed consistently.

The pore in cell membrane formed by gasdermin-N domains will elicit pyroptosis, but also generate hyperactive cells which possess lower amounts of GSDMD pores than pyroptotic cells [37]. During pyroptosis, cell membrane ruptured and cytosolic protein released, and the same with hyperactive cells. For instance, it has been confirmed that the pore-forming protein gasdermin D regulates IL-1 release from hyperactive macrophages [37]. It hints that GSDMD may become a high sensitivity index than other inflammatory biomarkers. Compared with LDH and IFN- γ , also acting as inflammatory biomarkers [38, 39], at the presence of *E. coli*, *S. aureus* and *Salmonella*, GSDMD displayed the most rapid and largest degree of growth tendency of GSDMD in the culture supernatant. In the previous report, after 24h the concentration of IL-27 in the mononuclear cells culture supernatants at the present presence of Mtb antigen began to increase [40]. But the concentration of GSDMD which began to increase after 1h changed faster and could make a contribution to early diagnosis. These showed that GSDMD diagnosed infectious pneumonia with a higher sensitivity. Expressed by innate immune cells, IL-1 β has been demonstrated to play a role in many inflammatory diseases, as well as in different cancers [41]. The higher diagnostic sensitivity at the presence of PA might lie in the following reason. The *Pseudomonas aeruginosa* mannose sensitive haemagglutination strain (PA-MSHA)-primed dendritic cells (DCs) directed T cell differentiation and primed Th cell to Th1 by elevated secretion of IFN- γ [42]. In conclusion, under various kinds of pathologic status especially in the case of bacteria infection, the level of GSDMD changed quick and large variation amplitude, which improved the diagnostic sensitivity and the ability of early diagnosis. Meanwhile, for regulating the release of the proinflammatory cytokines IL-1 β and IL-18 and pyroptotic cell death, GSDMD would possess higher diagnostic specificity. Besides, GSDMD had an advantage in diagnostic specificity in bacteria infectious which was the main cause of pyroptosis.

We further examined the change in PE-GSDMD during bacterial pneumonia treatment with an antibiotic. The responder was gradually decreased from baseline during therapy, while nonresponders showed the opposite tendency in PE-GSDMD. The research revealed % of GSDMD change at day 4 could predict the treatment response at an early stage (AUC = 0.945, Specificity = 96.15%) and be better than other traditional indicators. The utility of procalcitonin (PCT)-guided antibiotic treatment of intensive care patients has been postulated [43]. There is research reported that the AUC of PCT clearance rate at 5 and 9 days were 0.648 and 0.729 on the therapeutic effect of ventilator-associated pneumonia [44]. As one of the important causes of toxic and side effects of some chemotherapy drugs, caspase-3 activation can trigger necrosis by cleaving GSDME [45]. This means that detection based on GSDME expression level can be used as a better tool for prognosis interpretation. Besides, it's difficult to repeatedly extract PE

from lung cancer patients. There are some limitations to our study. Firstly, the limited population was enrolled in this study which may lead to bias. Also, it's difficult to rule out the misclassification of pleural fluid, especially the transudate group and PPE effusion and the collection of PE is also an invasive test. Moreover, further study needs to be conducted to clarify the normal level of serum GSDMD.

Conclusions

In brief, we found under infection and some other diseases a mass of GSDMD was secreted from NCs and released into PE rapidly. And our study firstly manifests that pleural fluid GSDMD can be an effective novel biomarker for the early differential diagnosis of PE.

Abbreviations

GSDMD: Gasdermin D; PE: pleural effusion; TPE: tuberculous pleural effusion; PPE: parapneumonic pleural effusion; MPE:malignant pleural effusion; ROC: receiver operating characteristic; NCs: Nucleated cells; ADA: adenosine deaminase; LDH: lactate dehydrogenase; Mtb: Mycobacterium tuberculosis; NT-GSDMD: gasdermin-N domain; IL-1 β : interleukin-1 β ; NSCLC: non-small cell lung cancer; NCCN: National Comprehensive Cancer Network; *E.coil*: *Escherichia coli*, *S.aureus*: *Staphylococcus aureus*, *PA*: *Pseudomonas aeruginosa*; LPS: lipopolysaccharide; PRR: pattern recognition receptors; PAMP: pathogen-associated molecular patterns; PA-MSHA: pseudomonas aeruginosa mannose sensitive haemagglutination strain; DCs: dendritic cells; PCT: procalcitonin.

Declarations

Acknowledgements

None.

Authors' contributions

Pu Li and Jing Shi designed and performed experiments and prepared the figures; Yuan Yuan, Jing Shi, Lijing Zhou, Bo Wang, Li Jun Zhang, Liang Duan, Qing Zhao and Qin Hu performed experiments; Xiaolan Zhou analyzed the data. Weixian Chen, Xuemei Peng and Liang Duan contributed to the experimental design and edited the manuscript; Pu Li supervised all research. Pu Li, Yuan Yuan and Lijing Zhou wrote the manuscript. All authors discussed the results and commented on the manuscript.

Funding

This work was partially sponsored by Grants from 'The Outstanding Young Talents Plan of the Second Hospital of Chongqing Medical University (Pu Li)', and from 'the Chongqing Science and Technology Bureau (General Project: cstc2020jcyj-msxm0226 and cstc2019jcyj-msxmX0349)'.

Data availability

The datasets generated during and/or analyzed during the current study are available from the corresponding author on reasonable request.

Ethics approval and consent to participate

All procedures followed were in accordance with the ethical standards of the responsible committee on human experimentation (institutional and national) and with the Helsinki Declaration of 1975, as revised in 2008. The study had been approved by the medical ethics committee of the Second Affiliated Hospital of Chongqing Medical University. Informed consent was obtained from all patients for being included in the study.

Consent for publication

All authors approved the manuscript and gave their consent for publication.

Competing interests

The authors declare that they have no competing interests.

Author details

¹ Department of Laboratory Medicine, the Second Hospital of Chongqing Medical University, 8602363693193, Chongqing 400010, China.

² Department of Laboratory Medicine, the First Hospital of Chongqing Medical University, 8602363693193, Chongqing 400042, China.

³ Department of Medical record management, the Second Hospital of Chongqing Medical University, 8602363693193, Chongqing 400010, China.

⁴ Laboratory medical college, Chongqing Medical University, 8602363693193, Chongqing 400010, China.

⁵ Department of Neurology, Chongqing People's Hospital, 8602363693193, Chongqing 400010, China.

References

1. Feller-Kopman D, Light R. Pleural Disease. *Engl. J. Med.* 2018, 378: 740-751.
2. Lee Jaehee, YooSeung Soo, Lee Shin Yup et al. Pleural fluid adenosine deaminase/serum C-reactive protein ratio for the differentiation of tuberculous and parapneumonic effusions with neutrophilic predominance and high adenosine deaminase levels. *Infection*, 2017, 45: 59-65.
3. Liang QL, Shi HZ, Wang K, Qin SM, Qin XJ. Diagnostic accuracy of adenosine deaminase in tuberculous pleurisy: A meta-analysis. *Respir Med.* 2008 May; 102 (5): 744-754.

4. Wang Jinlin, LiuJun, XieXiaohong. et al. The pleural fluid lactate dehydrogenase/adenosine deaminase ratio differentiates between tuberculous and parapneumonic pleural effusions. *BMC Pulm Med*, 2017, 17: 168.
5. Wang Jinlin, Liu Jun, XieXiaohong, et al. The pleural fluid lactate dehydrogenase/adenosine deaminase ratio differentiates between tuberculous and parapneumonic pleural effusions. *BMC Pulm Med*, 2017, 17: 168.
6. Man SM, Karki R, Kanneganti TD. Molecular mechanisms and functions of pyroptosis, inflammatory caspases and inflammasomes in infectious diseases. *Immunol Rev.*2017;277 (1): 61-75.
7. Jorgensen I, Miao EA. Pyroptotic cell death defends against intracellular pathogens. *Immunol Rev.* 2015;265 (1): 130-142.
8. Kovacs SB, Miao EA. Gasdermins: effectors of pyroptosis. *Trends Cell Biol.* 2017;27 (9): 673-684. DOI: 10.1016/j.tcb.2017. 05.005.
9. Broz, P., and V.M. Dixit. Inflammasomes: mechanism of assembly, regulation and signaling. *Nat. Rev. Immunol*, 2016, 16:407-420.
10. Gao Jianwei, QiuXiangyu, XiGuangmin et al. Downregulation of GSDMD attenuates tumor proliferation via the intrinsic mitochondrial apoptotic pathway and inhibition of EGFR/Akt signaling and predicts a good prognosis in non-small cell lung cancer. *Oncol. Rep.*, 2018, 40: 1971-1984.
11. Cheng KwongTai, XiongShiqin, YeZhiming et al. Caspase-11-mediated endothelial pyroptosis underlies endotoxemia-induced lung injury. *J. Clin. Invest.*, 2017, 127: 4124-4135.
12. Gong Zhen, KuangZhongmei, Li Hui, et al. Regulation of host cell pyroptosis and cytokines production by *Mycobacterium tuberculosis* effector PPE60 requires LUBAC mediated NF- κ B signaling. *Cell. Immunol.*, 2019, 335: 41-50.
13. Kalil Andre C, Metersky Mark L, Klompas Michael et al. Management of Adults With Hospital-acquired and Ventilator-associated Pneumonia: 2016 Clinical Practice Guidelines by the Infectious Diseases Society of America and the American Thoracic Society. *Clin. Infect, Dis.*, 2016, 63: e61-e111.
14. Antibacterial drug clinical trials technical guidelines' writing group. Guidance for clinical trials of antibacterial drugs. *Chin J Clin Pharmacol.* 2014, 30 (9): 844-856.
15. XiongYuan, YeYuanyuan, Li Pu et al. Serum NOX2 as a new biomarker candidate for HBV-related disorders. *Am J Transl Res*, 2018, 10: 2350-2361.
16. Ding Jingjin, WangKun, Liu Wang et al. Erratum: Pore-forming activity and structural autoinhibition of the gasdermin family. *Nature*, 2016, 540: 150.
17. Shi J, Zhao Y, Wang K, et al. Cleavage of GSDMD by inflammatory caspases determines pyroptosis cell death. *Nature*, 2015, 526 (7575):660-665.
18. Yang Xinyu, ChengXiaoye, TangYiting, et al. Bacterial Endotoxin Activates the Coagulation Cascade through Gasdermin D-Dependent Phosphatidylserine Exposure. *Immunity*, 2019, 51: 983-996.e6.
19. Fogel N. Tuberculosis: a disease without boundaries. *Tuberculosis (Edinb)*, 2015,95 (5): 527-531.

20. Lerner TR, Borel S, Gutierrez MG. The innate immune response in human tuberculosis. *Cell Microbiol*, 2015,17 (9): 1277-1285.
21. Beckwith Kai S, Beckwith Marianne S, UllmannSindre, et al. Plasma membrane damage causes NLRP3 activation and pyroptosis during Mycobacterium tuberculosis infection. *Nat Commun*, 2020, 11: 2270.
22. Jin C, Flavell RA. Molecular mechanism of NLRP3 inflammasome activation. *J Clin Immunol*, 2010, 30 (5): 628-631.
23. Ma D, Liu XL, Fang F. Research progress on absent in melanoma 2 in defendant pathogenic microorganism invasion. *Chin J Clin Infect Dis*, 2016,9 (1): 87-91.
24. Jiang Z, Yao L, Hongge M, et al. miRNA-214 inhibits cellular proliferation and migration in glioma cells targeting Caspase-1 involved in pyroptosis. *Oncol Res*, 2017, 25 (6): 1009-1019.
25. Wang Y, Gao W, Shi X, et al. Chemotherapy drugs induce pyroptosis through Caspase-3 cleavage of a Gasdermin. *Nature*, 2017, 547(7661): 99-103.
26. Derangere V, Chevriaux A, Courtaut F, et al. Liver X receptor activation induces pyroptosis of human and murine colon cancer cells. *Cell Death Differ*, 2014, 21 (12): 1914-1924.
27. Cooper Sandra T, McNeil Paul L, Membrane Repair: Mechanisms and Pathophysiology. *Physiol. Rev.*, 2015, 95: 1205-40.
28. Liu, X., Zhang, Z., Ruan, J., Pan, Y., Magupalli, V.G., Wu, H., and Lieberman, J. Inflammasome activated gasdermin D causes pyroptosis by forming membrane pores. *Nature*. 2016 535, 153-158.
29. Wang Wen, Zhou Qiong, ZhaiKan et al. Diagnostic accuracy of interleukin 27 for tuberculous pleural effusion: two prospective studies and one meta-analysis. *Thorax*, 2018, 73: 240-247.
30. Tang Yimin, Zhang Juanjuan, Huang Huarong, et al. Pleural IFN- γ release assay combined with biomarkers distinguished effectively tuberculosis from malignant pleural effusion. *BMC Infect. Dis.*, 2019, 19: 55.
31. Chung W, Jung Y, Lee K et al. CXCR3 ligands in pleural fluid as markers for the diagnosis of tuberculous pleural effusion. *Int. J. Tuberc. Lung Dis*. 2017, 21: 1300-1306.
32. Shi Jing, LiPu, ZhouLijin, et al. Potential biomarkers for antidiastole of tuberculous and malignant pleural effusion by proteome analysis. *Biomark Med*, 2019, 13: 123-133.
33. Shi Jianjin, GaoWenqing, ShaoFeng, Pyroptosis: Gasdermin-Mediated Programmed Necrotic Cell Death. *Trends Biochem. Sci.*, 2017, 42: 245-254.
34. Wallach David, Kang Tae-Bong, Dillon Christopher P, et al. Programmed necrosis in inflammation: Toward identification of the effector molecules. *Science*, 2016, 352: aaf2154.
35. Ryu J-C, Kim M-J, Kwon Y et al. Neutrophil pyroptosis mediates pathology of *P. aeruginosa* lung infection in the absence of the NADPH oxidase NOX2. *Mucosal Immunol*, 2017, 10: 757-774.
36. Miao EA, Leaf IA, Treuting PM, et al. Caspase-1-induced pyroptosis is an innate immune effector mechanism against intracellular bacteria. *Nat Immunol*, 2010, 11(12): 1136-1142.

37. Evavold Charles L, RuanJianbin, TanYunhao et al. The Pore-Forming Protein Gasdermin D Regulates Interleukin-1 Secretion from Living Macrophages. *Immunity*, 2018, 48: 35-44.e6.
38. Liu Ta-Yu, Lee Wei-Ju, TsaiChih-Min, et al. Serum lactate dehydrogenase isoenzymes 4 plus 5 is a better biomarker than total lactate dehydrogenase for refractory *Mycoplasma pneumoniae* pneumonia in children. *PediatrNeonatology*, 2018, 59: 501-506.
39. Tang Yimin, ZhangJuanjuan, HuangHuarong, et al. Pleural IFN- γ release assay combined with biomarkers distinguished effectively tuberculosis from malignant pleural effusion. *BMC Infect. Dis.*, 2019, 19: 55.
40. Yang Wei-Bing, LiangQiu-Li, YeZhi-Jian, et al. Cell origins and diagnostic accuracy of interleukin 27 in pleural effusions. *PLoS ONE*, 2012, 7: e40450.
41. Zhang Weizhou, Borchering Nicholas, Kolb Ryan, IL-1 Signaling in Tumor Microenvironment. *Adv. Exp. Med. Biol.*, 2020, 1240: 1-23
42. Zhang Yunyan, Wang Hongtao, Li Youqiang et al. The *Pseudomonas aeruginosa* Mannose Sensitive Hemagglutination Strain (PA-MSHA) Induces a Th1-Polarizing Phenotype by Promoting Human Dendritic Cells Maturation. *Indian J. Microbiol.*, 2014, 54: 163-9.
43. de Jong Evelien, vanOers Jos A, Beishuizen Albertus et al. Efficacy and safety of procalcitonin guidance in reducing the duration of antibiotic treatment in critically ill patients: a randomized, controlled, open-label trial. *Lancet Infect Dis*, 2016, 16: 819-827.
44. AbulaAbudusalamu, WangYi, Ma Long et al. [The application value of the procalcitonin clearance rate on therapeutic effect and prognosis of ventilator associated pneumonia. *Zhonghua Wei Zhong Bing Ji Jiu Yi Xue*, 2014, 26: 780-4.
45. Wang Yupeng, GaoWenqing, ShiXuyan, et al. Chemotherapy drugs induce pyroptosis through caspase-3 cleavage of a gasdermin. *Nature*, 2017, 547: 99-103.

Tables

Table 1. Biochemical and cytological characteristics in pleural effusions*

Characteristics	Pleural effusions			
	TPE	MPE	PPE	Control
Patients, No.	82	80	92	81
Males/Females	42/40	43/37	49/43	45/36
Age (years)	50.50±15.69	61.55±10.67	53.50±13.72	53.81±14.52
GSDMD (ng/mL)	49.38±21.17	27.96±14.17	26.25±13.37	4.70±3.52
LDH (U/L)	378.97±287.73	393.13±319.35	181.47±82.79	134.85±121.96
ADA (U/L)	37.09±15.91	21.88±12.17	14.25±6.60	8.06±4.81
nucleated cell counts,*10 ⁶ /L	4078.55±2842.70	3863.00±3183.23	942.98±480.23	101.26±53.94

LDH: lactate dehydrogenase; ADA: adenosine deaminase; TPE: tuberculous pleural effusion; MPE: malignant pleural effusion; PPE: parapneumonic pleural effusion; *Values are presented as mean ± SD.

Table 2. The value of AUC of biomarkers for pleural effusion antidiastole.

Group Biomarker	Control <i>versus</i> TPE	Control <i>versus</i> MPE	Control <i>versus</i> PPE	TPE <i>versus</i> PPE	TPE <i>versus</i> MPE	PPE <i>versus</i> MPE
GSDMD (Sensitivity, %)	0.990 (100.0)	0.963 (95.0)	0.967 (97.8)	0.885 (88.0)	0.848 (90.0)	0.557 (45.0)
ADA (Sensitivity, %)	0.937 (79.3)	0.896 (81.3)	0.771 (83.7)	0.863 (96.7)	0.758 (82.5)	0.713 (70.0)
LDH (Sensitivity, %)	0.872 (78.0)	0.864 (81.3)	0.710 (69.6)	0.802 (84.8)	0.536 (57.5)	0.747 (84.8)
Combination	0.998	0.980	0.973	0.968	0.863	0.756

LDH: lactate dehydrogenase; ADA: adenosine deaminase; TPE: tuberculous pleural effusion; MPE: malignant pleural effusion; PPE: parapneumonic pleural effusion

Table 3. Diagnostic value of combined detection of GSDMD, ADA and LDH for pleural effusion antidiastole.

	Control <i>versus</i> TPE	Control <i>versus</i> MPE	Control <i>versus</i> PPE	TPE <i>versus</i> PPE
Area under curve (95% confidence interval)	0.998 (0.995-1.000)	0.980 (0.960-0.999)	0.973 (0.945-1.000)	0.968 (0.942-0.994)
<i>P</i> value	<0.0001	<0.0001	<0.0001	<0.0001
Sensitivity, %	100.0	94.9	95.7	87.8
Specificity, %	97.5	96.2	96.3	98.9

LDH: lactate dehydrogenase; ADA: adenosine deaminase; TPE: tuberculous pleural effusion; MPE: malignant pleural effusion; PPE: parapneumonic pleural effusion

Table 4. The trend of GSDMD changes in PPE due to therapeutic effect.

	The efficacy group (n=26)		The non-efficacy group (n=14)		<i>P</i>
	Mean (ng/mL)	SD (ng/mL)	Mean (ng/mL)	SD (ng/mL)	
PE-GSDMD activity					
Baseline	35.28	18.72	26.42	11.09	0.1138
Day2	27.72	14.53	25.45	7.57	0.5898
Day 4	15.25	12.48	35.01	14.78	<0.0001
% of GSDMD change from baseline					
Day 2	-18.82	19.64	13.67	63.71	0.0205
Day 4	-59.15	25.61	47.13	68.77	<0.0001

GSDMD: Gasdermin D; PPE: parapneumonic pleural effusion.

Figures

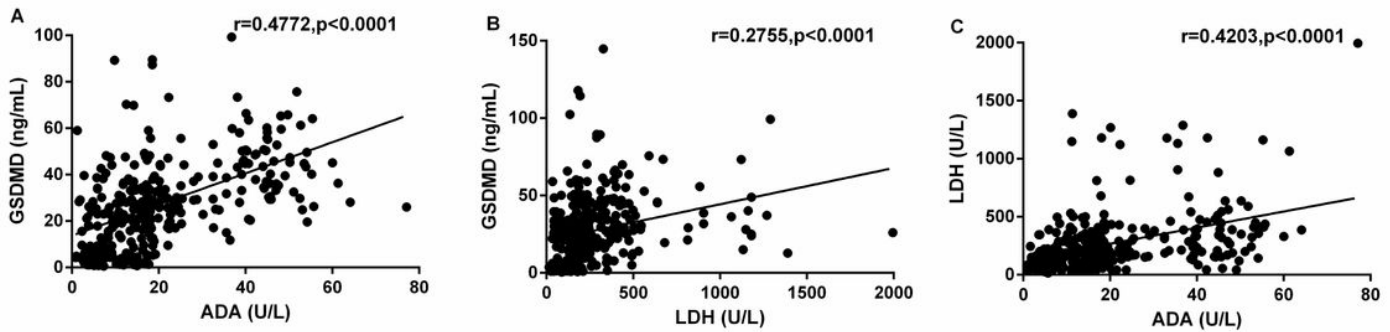


Figure 1

Correlation analysis of GSDMD with ADA (A), GSDMD with LDH (B) and ADA with LDH (C). (n=335). ADA: adenosine deaminase; LDH: lactate dehydrogenase; Correlations were determined by Pearson correlation coefficients.

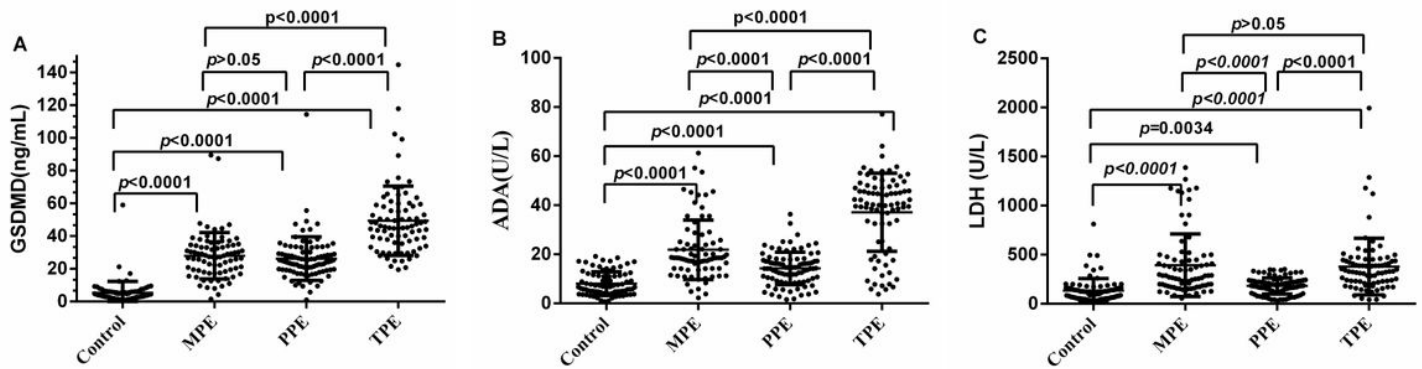


Figure 2

Comparisons of GSDMD (A), ADA (B) and LDH (C) concentrations with TPE (n=82), MPE (n=80), PPE (n=93) and transudative pleural effusion (n=81). TPE: tuberculous pleural effusion; MPE: malignant pleural effusion; PPE: parapneumonic pleural effusion; Horizontal bars indicate means. Statistical analysis was done by one-way analysis of variance.

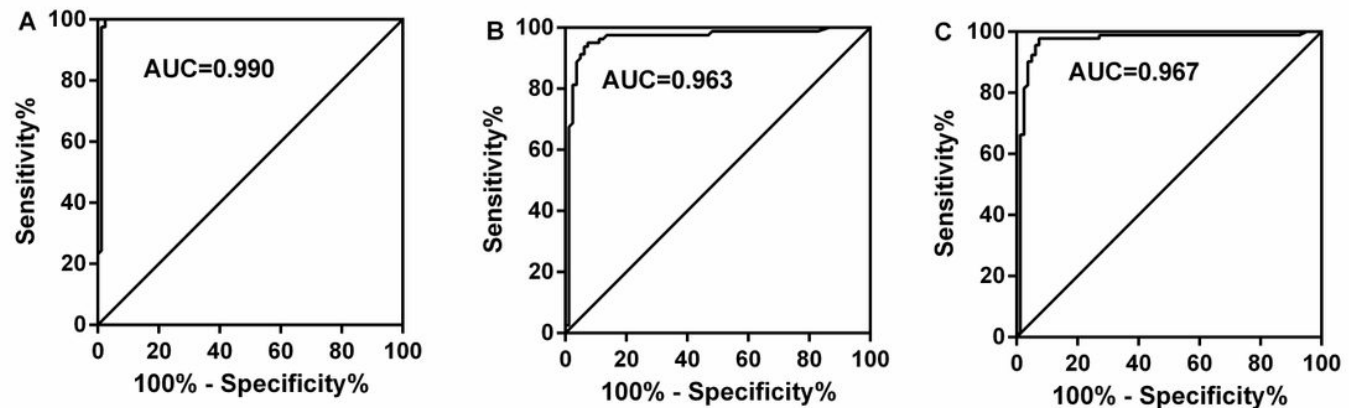


Figure 3

Receiver operating characteristic curves of GSDMD for differential diagnosis of Control (n=81) versus TPE (n=82) (A), of Control (n=81) versus MPE (n=80) (B), and of Control (n=81) versus PPE (n=92) (C). TPE: tuberculous pleural effusion; MPE: malignant pleural effusion; PPE: parapneumonic pleural effusion; AUC: area under curve.

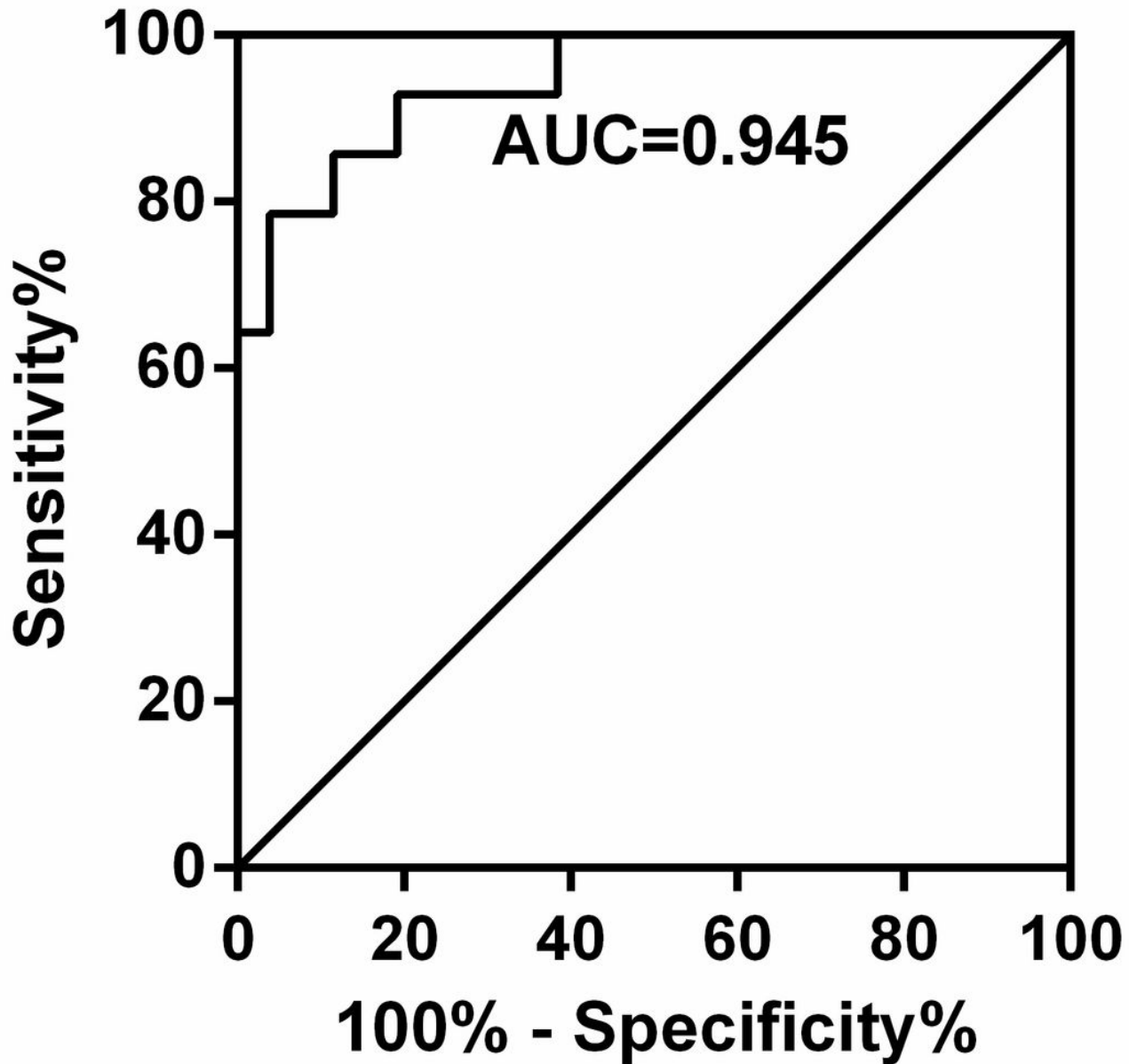


Figure 4

Receiver operating characteristic curves for the percentage change in PE-GSDMD at day 4 in predicting which patients would have a partial response or stable disease.

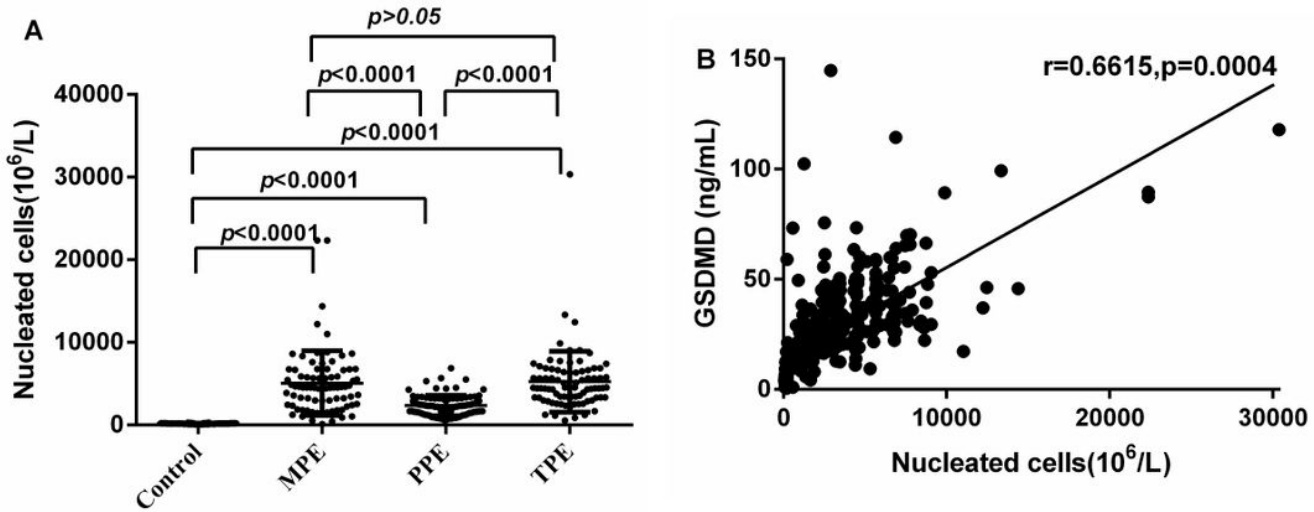


Figure 5

Comparisons of nucleated cells count in pleural effusion in Control (n=81), MPE (n=80), TPE (n=82), PPE (n=92) groups (A) and concentrations of GSDMD correlated with the numbers of nucleated cells in pleural effusion (n=335) (B). TPE: tuberculous pleural effusion; MPE: malignant pleural effusion; PPE: parapneumonic pleural effusion; Horizontal bars indicate means. Statistical analysis was done by one-way analysis of variance. Correlations were determined by Pearson correlation coefficients.

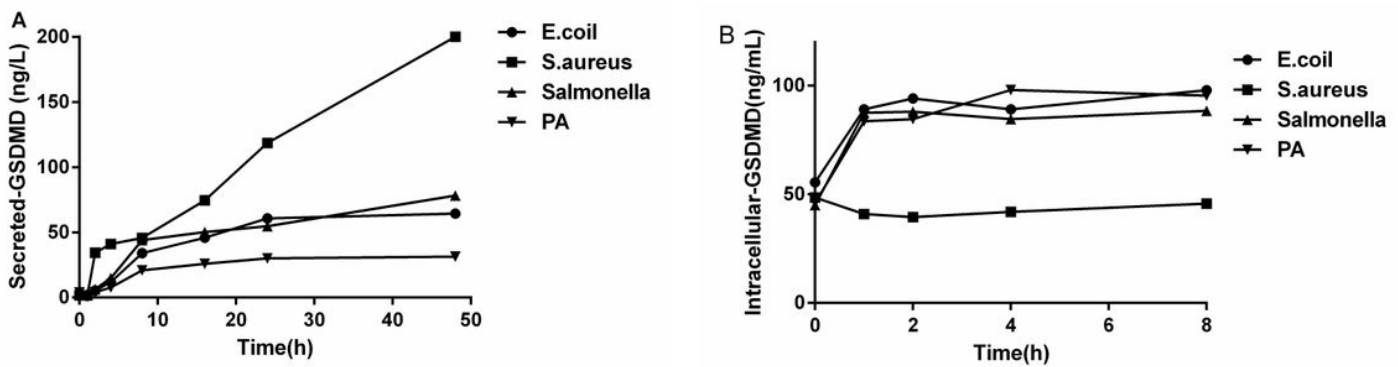


Figure 6

The concentration of the secreted (A)/intracellular (B)-GSDMD by nucleated cells was cultured respectively in vitro in the presence of bacteria E.coli: Escherichia coli; S.aureus: Staphylococcus aureus; PA: Pseudomonas aeruginosa.

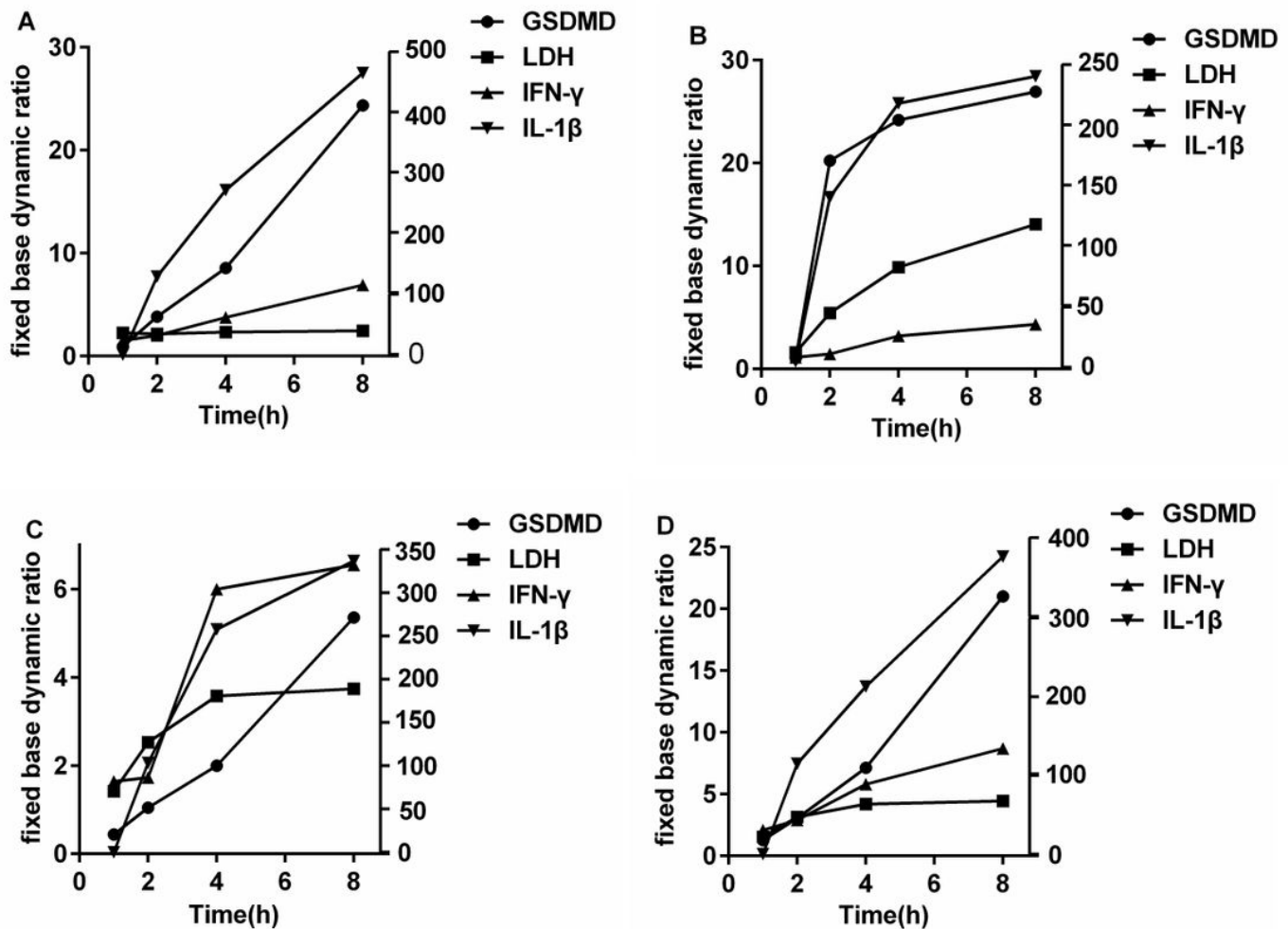


Figure 7

Trend analysis (fixed base dynamic ratio= assay value/fixed value (Control)) of GSDMD, LDH, IFN- γ and IL-1 β in culture supernatants at the presence of E.coli (A), S.aureus (B), PA (C) and Salmonella (D). LDH: lactate dehydrogenase; IFN- γ : interferon- γ ; IL-1 β : interleukin-1 β ; E.coli: Escherichia coli; S.aureus: Staphylococcus aureus

Supplementary Files

This is a list of supplementary files associated with this preprint. Click to download.

- [AdisRapidOpenAccessDisclosureForm.pdf](#)
- [keysummarypoints.doc](#)